System Reliability Benefits of Repetitive Framing in Cold-Formed Steel Floor Systems

Brooks H. Smith, P.E., M.ASCE[1]; Aritra Chatterjee, Ph.D., S.M.ASCE[2]; Sanjay R. Arwade, Ph.D., M.ASCE[3]; Cristopher D. Moen, Ph.D., M.ASCE[4]; and Benjamin W. Schafer, Ph.D., P.E., M.ASCE[5]

Abstract: Typical cold-formed steel floor systems involve many repetitive joist members laid in parallel, yet the design specifications are based upon the reliability of individual members and fail to account for the potential benefits imparted by repetitive framing. A repetitive member factor, similar to that used in the United States National Design Specifications (NDS) for wood, could be used in cold-formed steel (CFS) design to recognize these benefits and allow for more economical and efficient design that does not compromise safety. This paper introduces and validates procedures based on Monte Carlo simulation for assessing the performance of repetitive floor systems under current code assumptions, and elastic and inelastic load redistribution mechanisms, and uses these procedures to examine two floor systems of varying complexity. Load redistribution is found to provide a benefit of at least 30% to the capacity of the floor system based on a target reliability index of 2.5 and therefore justifies applying a 1.25 factor to the design of joist capacity for the systems studied. **DOI: 10.1061/(ASCE)ST.1943-541X.0002025.**

Author keywords: Repetitive member factor; Structural reliability; Design efficiency; Floor systems; Cold-formed steel.

Introduction

This paper investigates the role that system effects play in determining the reliability of cold-formed steel (CFS) floor systems that make use of repetitive framing. Monte Carlo simulation is used to evaluate the system reliability of such floor systems and define an allowable increase in design capacity that still results in the floor system achieving the target level of system reliability.

Component design methodology has existed for cold-formed steel for some time, but it is only in the last 20 years that full-building solutions, notably integrating seismic design, have been developed for CFS. Since an initial characterization of wood sheathed CFS shear walls by Serrette et al. (1997), research has focused upon experimental studies of shear walls (Landolfo et al. 2006), fasteners (Fiorino et al. 2007), and prototype buildings (Iuorio et al. 2014). Numerical models (Fülöp and Dubina 2004) and complete seismic design procedures (Dubina 2008) have been developed, and the recent popularity of CFS residential structures in Australia and China have led to growing data on lateral force resisting systems for the material (Gad et al. 1999; Li et al. 2012).

The positive or negative effects of having multiple interconnected structural components acting together is known as the system effect, and can profoundly alter the reliability of the system relative to the reliability of the components. Although research in system reliability has rarely focused specifically upon CFS, important contributions have included studies of load paths (Moses 1982; Rashedi and Moses 1988), redundancy, load distribution and duration (Rosowsky and Ellingwood 1991), and uncertainty in demands and capacities (e.g., Ellingwood and Kinali 2009; Chatterjee et al. 2017). Among other things, system reliability depends upon the load-deformation characteristics of each component and the nature of their interconnections (Hendawi and Frangopol 1994).

The United States National Design Specifications (NDS) for wood construction establishes a repetitive member factor that allows a 15% increase in the capacity of wood joists in a floor system that involves several identical members working in parallel (ANSI and AWC 2012). Cold-formed steel framing has many similarities to wood framing, but no similar allowance is made in current CFS specifications. In the NDS, the repetitive member factor is intended to include three effects: (1) elastic load sharing, (2) postelastic residual capacity, and (3) composite action between sheathing and joists (Rosowsky and Yu 2004; Verrill and Kretschmann 2010). Rosowsky and Ellingwood (1991) examined this longstanding repetitive member factor from a system reliability standpoint in and showed it to be reasonable if load duration effects for the wood are considered (Foschi and Yao 1989). This paper addresses the first two system effects for two representative CFS floor systems, using system reliability methods similar to the work of Rosowsky and Ellingwood (1991).

An efficient, approximate analysis algorithm was developed and implemented in *MATLAB* that is capable of rapid iterative load redistribution for a sheathing-covered CFS floor system with overall rectangular plan, parallel joists, arbitrary and variable joist spacing, and the presence of openings in the floor system. Joist capacities are calculated based on the 2012 American Iron and Steel Institute

[1]Research Fellow, Dept. of Civil and Environmental Engineering, Univ. of Massachusetts, 223 Marston Hall, Amherst, MA 01003 (corresponding author). ORCID: https://orcid.org/0000-0003-0887-0361. E-mail: Brooks.H.Smith@dartmouth.edu

[2]Graduate Research Assistant, Dept. of Civil and Environmental Engineering, Virginia Polytechnic Institute and State Univ., 200 Patton Hall, Blacksburg, VA 24061. E-mail: aritrac1@vt.edu

[3]Professor, Dept. of Civil and Environmental Engineering, Univ. of Massachusetts, 223 Marston Hall, Amherst, MA 01003. E-mail: arwade@umass.edu

[4]Professor, Dept. of Civil Engineering, Johns Hopkins Univ., 208 Latrobe Hall, Baltimore, MD 21218. E-mail: cmoen@jhu.edu

[5]Professor, Dept. of Civil Engineering, Johns Hopkins Univ., 208 Latrobe Hall, Baltimore, MD 21218. E-mail: schafer@jhu.edu

Note. This manuscript was submitted on June 15, 2017; approved on October 28, 2017; published online on April 10, 2018. Discussion period open until September 10, 2018; separate discussions must be submitted for individual papers. This paper is part of the ***Journal of Structural Engineering***, © ASCE, ISSN 0733-9445.

S100-12 design specification for the United States (AISI 2012), whereas demands are determined by treating sheathing panels and joists as beam elements. Live loads for the floor are taken as uniform as per ASCE 7-10 (ASCE and SEI 2010), assuming a typical commercial office building. This paper considered two floor systems, a regular floor with uniform joist spacing and no openings, and a rectangular floor with nonuniform joist spacing and openings. Both systems were developed from the layout of the building investigated and tested extensively at full scale for the project entitled "NEESR-CR: Enabling Performance-Based Seismic Design of Multi-Story Cold-Formed Steel Structures"—abbreviated as CFS-NEES (Schafer 2015; Peterman 2014; Peterman et al. 2014).

Characteristics of Floor Models

This paper uses two example floor systems to illustrate system effects on floor system reliability as a function of component reliability. The first is a simplified floor system used to develop basic insights into load sharing in CFS floor systems and the second is the upper-level framing system from the CFS-NEES building (Madsen et al. 2012; Nakata et al. 2012), included as an example of a typically designed floor system with some complicating features common in modern CFS design and construction. In the simplified system, the overall dimensions are round numbers, no floor openings are present, all joists run the full length of the floor, and joists are evenly spaced. The simplified system is included because it provides a clear illustration of the system effect of repetitive framing for a system in which nominally identical joists may share load after individual joist overload.

The CFS-NEES building (Madsen et al. 2012; Nakata et al. 2012) was professionally designed by Rob Madsen of Devco Engineering (Corvallis, Oregon) with input from the CFS-NEES research team led by one of the authors (Schafer) and from an industry advisory board comprising experienced cold-formed steel engineers in the United States and Canada. The design was intended to reflect current practice. The building has a rectangular floor plan with dimensions of 15.1 × 6.97 m (49.75 ft × 23 ft) and a total height of 5.83 m (19.25 ft).

The floor is ledger-framed, i.e., a ledger track is installed on the inside face of the wall studs and the floor joists are attached to this track with clip angles. Stud and joist spacing are not equal in ledger-framing. The top of the joist and the top of the wall are at the same elevation. Oriented strand board (OSB) sheathes the floor. The building uses OSB sheathed shear walls for the lateral force resisting system. A design narrative, complete calculations, and full drawings are available for the building (Madsen et al. 2012; Nakata et al. 2012).

The simplified floor was based on the CFS-NEES floor in that the overall plan dimensions are similar and the same joist size and sheathing system is used throughout. The overall dimensions, however, were regularized to a standard 7.32 × 14.63 m (24 × 48 ft), and all openings and cutouts were neglected so that all joists had the same length of 7.32 m (24 ft) and joist spacing of 0.61 m (2 ft) (Fig. 1).

The CFS-NEES floor system measures 14.86 × 6.67 m (48.75 × 21.88 ft) in joist dimensions, from end to end and from center to center of the outermost joists. There is a cutout in the northwest corner measuring 4.50 × 1.03 m (14.75 × 3.39 ft), and to accommodate the typical 0.61-m (2-ft) on-center joist spacing along the cutout, there are two joists with a narrower spacing of 0.23 m (0.75 ft) at 4.27 m (14 ft) and 4.50 m (14.75 ft) from the outer edge. Additionally, there is an opening in the eastern half of the floor, measuring 2.44 × 3.00 m (8.00 × 9.83 ft), with the southeastern corner located 3.05 m (10 ft) west and 1.50 m (4.92 ft) north of the floor edge (Fig. 2).

As described elsewhere (Smith et al. 2016), the CFS-NEES building has as-designed demand:capacity (d/c) ratios that vary widely due to the decision to specify a single joist size throughout the somewhat irregular floorplan. The maximum factored demand:capacity ratio is 0.91, indicating a high level of efficiency in the critical joist relative to the maximum allowable value of 1.0. Flexural capacity (considering local buckling) is typically the controlling limit state for the joists. Unfactored mean demand:capacity ratios range from 0.06 to 0.33 indicating the substantial reserve capacity present in the floor system. To be consistent with the analysis and redistribution methods used here, joist demands were calculated by assuming that the sheathing boards act as flexible beams simply supported on the joists. Therefore, due to the staggered OSB arrangement (Figs. 1 and 2) d/c ratios are not uniform but vary slightly in an alternating pattern even in the simplified system.

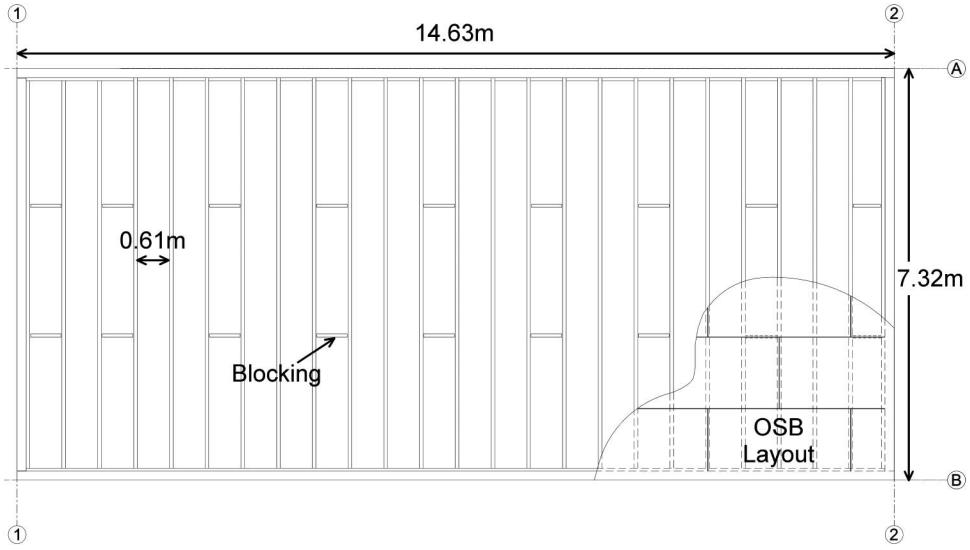

Fig. 1. Simplified floor system plan showing overall dimensions, joist spacing, ledger/header locations, blocking, and OSB sheathing layout

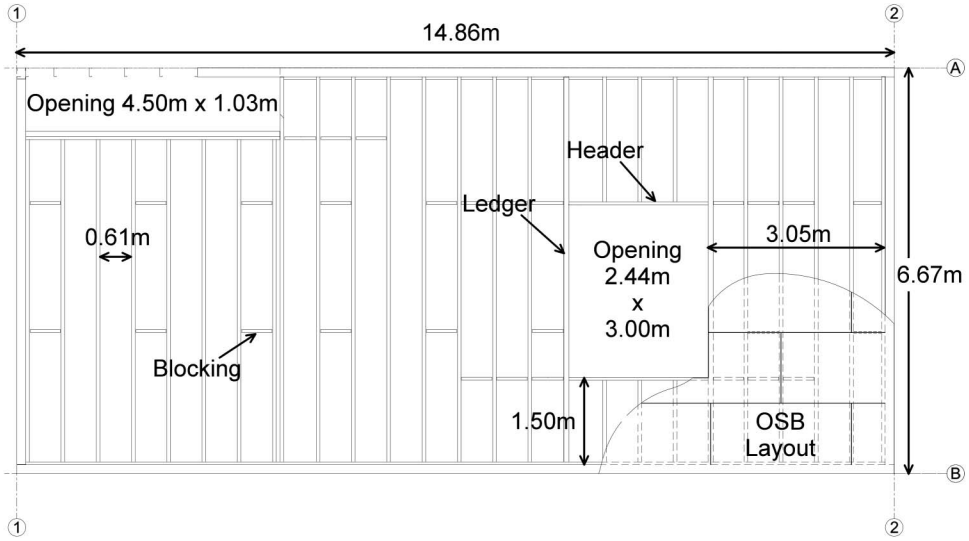

Fig. 2. CFS-NEES floor plan showing overall dimensions, joist spacing, ledger/header locations, blocking, and OSB sheathing layout along with openings

Simplified Floor Analysis Methodology

Researchers sometimes examine load redistribution using a finely-meshed, nonlinear finite-element analysis model of a single building (Agarwal and Varma 2014; Collins et al. 2005), but that approach comes with high computational expense. This study required the ability to perform thousands of diverse simulations rapidly, and although a handful of other similar studies exist (Rosowsky and Ellingwood 1992; Izzuddin et al. 2008), no commonly accepted approach to efficient assessment of load redistribution exists.

In this paper, the simulation analysis methodology relies upon the assumption that the joists and sheathing boards act as Euler-Bernoulli beams with the joists treated as single-span beams and the sheathing boards treated as multispan continuous beams with the joists playing the role of the support points. This method essentially treats the floor as an assembly of orthogonal beams in which the sheathing panels are supported by the joists, the joists are supported by the end ledgers, and the gravity load on the floor flows through the sheathing into the joists. The reactions provided to the sheathing boards by the joists are then treated as a series of partially distributed uniform loads along the length of the supporting joists. This method implies three key assumptions regarding the behavior of the sheathing boards: attachment to the joists is treated as pinned; two-way action of the sheathing boards at the perimeter of the floor, where one edge of the panel may bear directly on the track, is neglected; and the Poisson stiffening effect on the platelike sheathing boards is ignored.

Because of these simplifying assumptions, joist analysis becomes a problem of computing bending moments for an end-supported beam with piecewise constant applied gravity load. This allows efficient and repeated simulations such as those required in Monte Carlo simulation.

Modeling the sheathing panels as beams allows for load-sharing between parallel joists. Load sharing occurs under elastic deformations as the sheathing panels distribute gravity load to multiple joists. Once a joist reaches its moment capacity, additional load is assumed to be distributed to parallel joists through the beamlike action of the sheathing panels.

Inelastic Load Redistribution Theory

When the demand on a joist generated by the gravity load exceeds the joist's capacity, the excess demand is redistributed to parallel joists through beamlike action of the sheathing boards. Therefore the unfactored demand:capacity ratios are calculated using Load and Resistance Factor Design (LRFD) with safety factors removed or set equal to 1.0 (described in more detail subsequently). The load redistribution method identifies any joist that has a specific d/c ratio greater than 1, indicating overload, and attempts to redistribute excess load to other joists that share at least one sheathing board with the overloaded joist. This procedure assumes an elastic-perfectly plastic overall response for the joists in which the entirety of the overload must be carried by other joists but the overloaded joist continues to be able to carry its full capacity, and neglects geometric effects in which the downward displacement of an overloaded joist may affect sheathing board reactions. Ayhan and Schafer (2017) studied and characterized the ductility of CFS joists based on local and distortional cross-section slenderness. Large classes of CFS beams are capable of significant redistribution, particularly thicker joists that are primarily selected due to deflection considerations, but not all CFS beams can provide large plastic redistribution, a limitation that needs to be considered during any implementation of this work. The algorithm used for load redistribution, which uses superposition of sheathing board geometries with and without overloaded joists, is most easily explained through a numerical example, as given in the following example.

Example: Multiple Overcapacity Joists

This example is based upon a four-span continuous sheathing board [1.22×2.44 m (4×8 ft)] with joists spaced at 0.61 m (2 ft) on-center (Fig. 3), as is typical in the floor systems examined.

For simplicity, this example illustrates redistribution for only a single sheathing board. In the actual implementation, this same process is iterated for every sheathing board in the floor system until an equilibrium solution is reached, or until equilibrium convergence fails, in which case the floor system is considered to have failed in a system sense. Effects of this iteration for the entire floor system are discussed after the example in the next subsection.

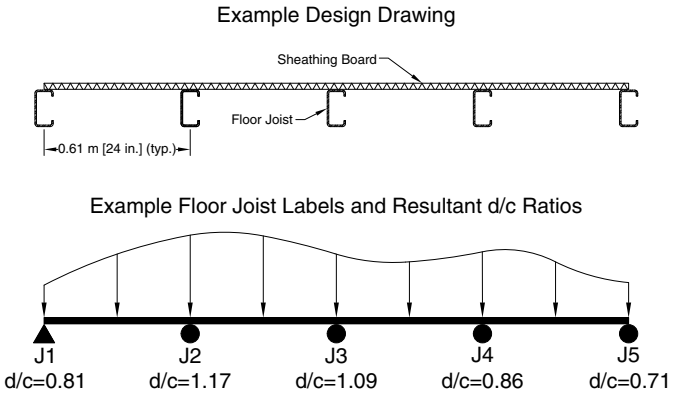

Fig. 3. Beam idealization of sheathing board as referenced throughout the example; sheathing board [1.22×2.44 m (4×8 ft)] is supported by five evenly spaced joists [0.61 m (2 ft) on-center], J1–J5; arbitrary load distribution is shown although this paper assumes piecewise constant distributed loads; the analysis method is applicable to arbitrary distributed and point loads as would arise if, for example, the load were modeled as a continuously varying random field

Fig. 3 shows an illustrative set of unfactored demand:capacity ratios, with J2 being loaded to 17% overcapacity and J3 being loaded to 9% overcapacity. Variability in d/c arises from variation in joist capacity; spatial variation in loading; or the fact that, when modeled as continuous beams, the sheathing transmits different fractions of the load to each supporting joist.

In this example, 17% of the load must be redistributed off J2, and 9% of the load must be redistributed off J3 in order to achieve an equilibrium state. The first iteration in finding an equilibrium solution is to analyze the beam using the superposition of three elastic solutions corresponding to the case in which J1–J5 are intact, the case in which J3 has reached its capacity and ceases to carry additional load, and the case in which both J2 and J3 have reached capacity and cease to carry additional load (Fig. 4). The three solutions in the superposition are proportioned according to the fraction of the total load assumed to be carried in the given configuration. These proportions are built into the changes in d/c shown in the figure. As load is applied, it is assumed that first all joists are fully intact, then the joist with the highest d/c ratio (J2, with $d/c = 1.17$) yields, redistributing its load, and finally joist J3 also yields, with the loads from both J2 and J3 then both redistributing.

Note that J3 remains overloaded ($J3 = 1.03 > 1.0$) even after the initial redistribution iteration. This is because the weights in Fig. 4 are computed based on the d/c ratios prior to the first iteration of redistribution. A second iteration of load redistribution would then be performed (Fig. 5). For this second iteration only two configurations need to be superimposed, one with all joists J1–J5 intact and one with J3 removed to represent its overloaded state.

After the second iteration, J2 ($R2 = 1.01 > 1.0$) is again overcapacity. Further iteration is performed until all d/c ratios are less than 1.005, resulting in no joist being overloaded by more than 0.5% of the capacity, or until the system fails to converge to an approximate equilibrium configuration, in which case the floor system is assumed to have undergone system failure. Physically, this process may be thought of as follows: an overloaded joist would exceed its yield moment and start to deform plastically. As the overloaded joist deforms, the bending stiffness of the sheathing board would force neighboring joists to take up more of the load while reducing the load on the overloaded joist until equilibrium is reached.

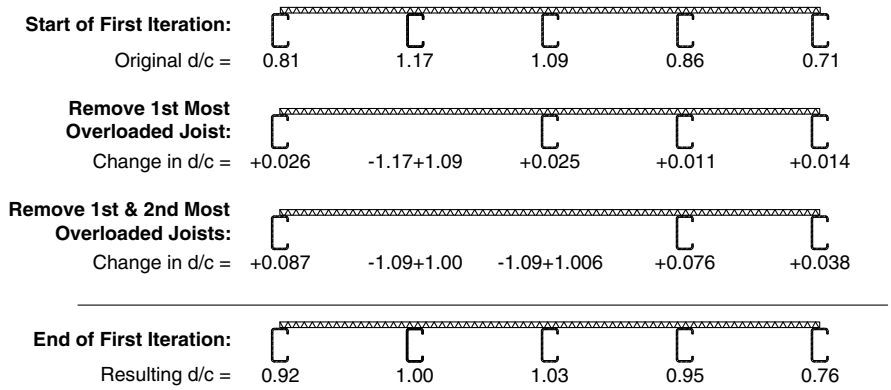

Fig. 4. First iteration of example, with two overcapacity joists

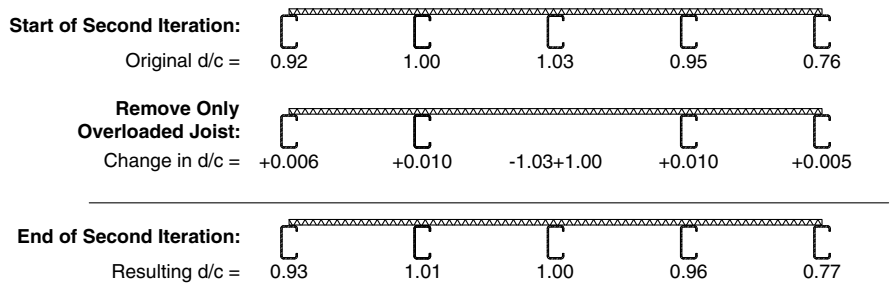

Fig. 5. Second iteration of example, after one of two overcapacity joists has already been corrected

Floor System Iteration

The preceding example illustrates the methodology for a single sheathing board, but a full analysis of the floor system redistribution requires treatment of all sheathing boards and joists in an iterative procedure (Fig. 6). Some key features of this procedure are: joist demands are not updated after each sheathing board redistribution, but only after analysis of all sheathing boards in the floor system; redistribution for each sheathing board is iterative ("Inelastic Load Redistribution Theory") and is controlled by an equilibrium tolerance of 0.5% of joist capacity; the overall iterative procedure is controlled by a threshold number of iterations after which, if a redistributed equilibrium configuration is not reached with no joists overloaded ($d/c \leq 1$), the floor system is assumed to have failed.

The opening in the CFS-NEES model also adds headers and carriers to the model. Within the analysis algorithm, carriers are treated exactly as joists, except that point loads equivalent to the header end reactions are also added by the principle of superposition. Furthermore, headers are assumed to carry no load directly from the sheathing boards, and instead carry only point loads equal to the end reactions of the joists connected to the headers. This assumption is in line with the treatment of sheathing boards as one-way beams and should not affect the total load carried by the headers. However, the loads on headers and their consequent point load reactions on the carriers are not possible to redistribute, although failures of these members are still considered in the algorithm. Such failures account for some instances of floor systems for which load redistribution was unable to prevent the floor system from failing.

Calculation of Demand to Capacity Ratios

The redistribution algorithm used here relies on the ratio of demand to capacity of a joist to determine when a joist is overloaded and a redistribution path must be sought. To calculate demand, gravity load combinations are based upon Load and Resistance Factor Design. Joist capacity is calculated in keeping with current practice in the United States cold-formed steel construction industry (AISI 2012) by checking for bending, distortional buckling, shear, and web crippling. Limit states considering combined bending and web crippling, and combined bending and shear failures, were checked according to procedures described in Smith et al. (2016) but these limits were not exceeded in any simulated cases.

All code-based design calculations include load and resistance factors, and thus the final design calculations provide D_f and C_f, the factored demand and capacity, respectively. Additional calculation is required to obtain D_u and C_u, the unfactored demand and capacity of components, respectively, and then μ_D and μ_C, the mean demand and capacity, respectively. The mean values are needed in simulation of random capacity and demand (Fig. 6). Unfactored demand D_u is calculated by omitting load factors and unfactored capacity C_u is calculated according to $C_u = C_f/\phi$, where ϕ is the LRFD resistance factor for the given failure mode.

The ratio $D_u/C_u = 1.0$, however, does not represent the point at which failure occurs, only the point at which a certain failure probability occurs. Bias factors are still included in D_u, and material, fabrication, and professional factors are still included in C_u. To remove these factors, the mean demand is calculated as

$$\mu_D = \frac{D_u}{C_\phi} \tag{1}$$

where bias factor $C_\phi = 1.52$, as per AISI S100, Table F1 (AISI 2012); and the mean capacity is

$$\mu_c = C_u M_m F_m P_m \tag{2}$$

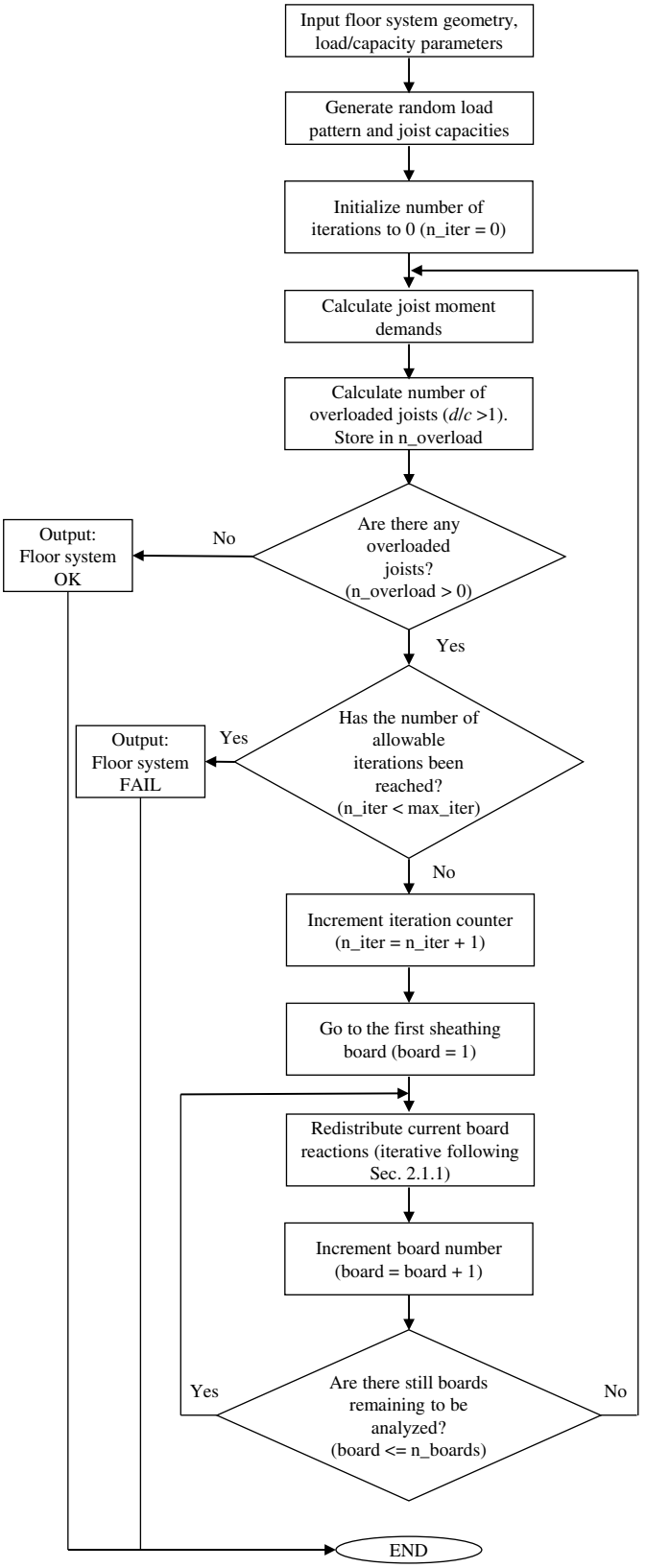

Fig. 6. Flowchart showing load redistribution algorithm for floor system

where for joists and carriers such as those used in this study, material factor $M_m = 1.1$; fabrication factor $F_m = 1.0$; and professional factor $P_m = 1.0$, as per AISI S100, Table F1 (AISI 2012).

Model Validation

The load redistribution method described in the Methodology section uses element deletion and superposition to calculate load distribution to joists in the case of joist overload. Therefore the goals of this validation are to ensure that the load distributions predicted by the simplified model for the virgin structure and for a structure with elements removed are accurate. A high-fidelity, three-dimensional (3D) finite-element model was developed (Chatterjee 2016), with the same floor geometry as described previously and using four-node shell elements (S4R) of approximately 2.5×2.5 cm (1×1 in) to model the joists. Linear elastic material properties were assumed. The 1200S250-97 joists were attached to 1200T200-97 tracks via spring elements representing screw fasteners, and blocking was added at the $1/3$ points. Uniformly distributed loads were applied to shell elements above the joists that represented the sheathing boards, and these were pinned to the top flange of the joists.

Because the most common failure mode for these joists was bending, the primary output values examined were joist moments, calculated by integrating the axial stress in the shell elements with their distance from the neutral axis. The maximum joist moments were compared between the high-fidelity *ABAQUS* model and the equivalent simplified analysis model.

Joist moments obtained from the simplified analysis method were found to agree with those obtained from the high-fidelity finite-element model to within an accuracy of approximately 5% for each of the eight models tested (the simplified floor system with all joists intact and seven cases in which single or multiple joists were removed from the model). Fig. 7 compares examples. This level of accuracy is taken to be acceptable for the purposes of examining load redistribution and system reliability effects.

Estimation of System Reliability

The key notion embodied in system reliability is that the reliability of a system of interconnected and interdependent components will not necessarily equal the reliability of any of the individual components. Indeed, the components will typically have widely varying reliabilities, and only in certain special cases can the system reliability be directly related to the reliability of any one individual component. The hypothesis of this study, consistent with the way repetitive framing is treated in timber framing (ANSI and AWC 2012; Rosowsky and Yu 2004; Verrill and Kretschmann 2010), is that the system effect in a CFS floor system will result in system reliabilities that are higher than the component reliabilities. Component reliability is driven primarily by four parameters, the means and variances of the component demand and capacity. Because demand is determined by design specifications, and variance of capacity is largely a function of manufacturing processes, the mean capacity is the only one of the four parameters directly under the control of the designer. Therefore this study selected the mean joist capacity as the parameter to vary in attempting to test the hypothesis that system effect in CFS floor systems is beneficial. If the hypothesis is found to be valid, the implication for designers is that joists with lower strength than are currently required could be specified and the floor system reliability would still attain target values.

To quantify the effect of load redistribution on system performance, a series of Monte Carlo simulations was performed at progressively decreasing reductions in the mean capacity of the joists. The goal of this series of simulations was to determine if mean joist capacity can be reduced relative to that required by component-by-component design and still result in the same target reliability for the overall system. This reduction in mean joist capacity is reflected in a system effect factor R_{sys} defined so that the mean joist capacity used in a simulation is

$$R_{\text{sys}} = \frac{\mu_{C,\text{design}}}{\mu_{C,\text{simulation}}} \tag{3}$$

where $\mu_{C,\text{simulation}}$ = mean component capacity needed to deliver target system reliability in Monte Carlo simulations that account for load redistribution; and $\mu_{C,\text{design}}$ = mean component capacity that results from standard component-by-component design. In other words, R_{sys} is a measure of how conservative the design is relative to what simulations indicate actually provides the intended system reliability. This relationship may also be expressed in its inverse as

$$R_{\text{sys}} = \frac{1}{1 - \bar{C}_{\text{reduction}}} \tag{4}$$

where $\bar{C}_{\text{reduction}}$ = amount by which the mean capacity of the joists may be reduced while maintaining the same system reliability. If the system effect is beneficial, then $R_{\text{sys}} > 1$ and joist capacity may be reduced. If the system effect is detrimental, as in the case of series systems, then $R_{\text{sys}} < 1$. In design of a repetitively framed floor system with a beneficial system effect, then, the resistance factor ϕ could be replaced in component design equations by ϕR_{sys}. This would result in a design that uses less material but achieves the same system reliability.

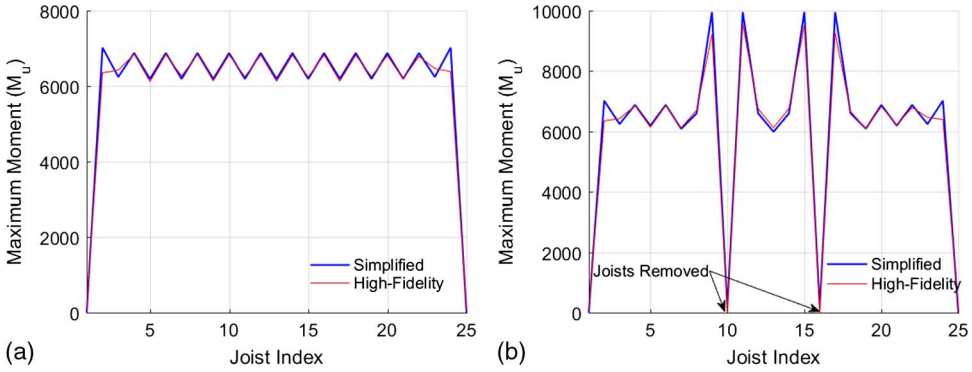

Fig. 7. Comparison between joist moment predictions from simplified beam element–based analysis model (*MATLAB*) and high-fidelity, 3D shell element–based finite-element model: (a) joist moments for intact simplified floor systems; (b) joist moments with two joists removed from model showing load transfer to adjacent joists due to bridging action of sheathing boards

Mean joist capacity was reduced in increments of 5%, from 100% (i.e., full capacity at the traditional design level) to 30%, corresponding to $1 < R_{sys} < 3.3$ (or $0.00 < \bar{C}_{reduction} < 0.70$). One thousand independent realizations of random floor loads and joist capacity were analyzed for each value of R_{sys}. Random input variables for the Monte Carlo simulations were all Gaussian and consisted of

1. Mean joist capacity, with a coefficient of variation (COV) of 0.15

$$\text{COV} = 0.15 = \sqrt{V_m^2 + V_F^2 + V_P^2} \tag{5}$$

   where V_m, V_F, and V_P = material, fabrication, and professional factors, respectively, for CFS joist members, as defined in AISI S100-12, Table F1 (AISI 2012). This random capacity was applied independently and with identical distribution to each joist in the system.
2. Live load, with a COV of 0.25, as defined by Galambos et al. (1982) and based upon AISI calculations.
3. Dead load, with a COV of 0.10, as similarly defined by Galambos et al. (1982) and based upon AISI calculations.

A suite of simulations was conducted to cover a range of floor system configurations, joist end conditions, and live load variation patterns. Specifically, the following cases were considered (Fig. 8):

1. Floor system configuration: Simplified floor system and CFS-NEES floor system.
2. Joist end fixities: Pinned and fully fixed. Code-based calculations assumed pin connections for all floor members, but some degree of partial restraint would have been provided by the end connection. A fully fixed end condition was included to indicate the possible maximum effect of joist end fixity on system response.
3. Live load variation pattern:
   a. Live load was assumed to be constant and independent and identically distributed over strips of the floor area corresponding to the tributary area of the joists.
   b. Live load was assumed constant and independent and identically distributed over square patches of the floor area [1.23 × 1.23 m (4 × 4 ft)]. This area was selected to be consistent with correlation areas for live load variation as observed and recommended by, e.g., McGuire and Cornell (1974).

Live load variation Pattern a reflects code assumptions, in which member loads are random with the given COVs over the entire length of an individual member and Pattern b is intended to reflect actual, physical patterns of live load variation more accurately.

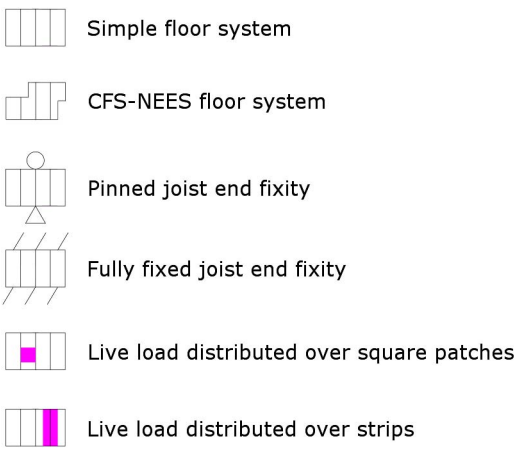

Fig. 8. Legend of icons used in subsequent figures

Summary of Assumptions

In order to set the stage for the "Results" section, although key assumptions were each discussed in detail previously, major assumptions are summarized as follows:

1. Composite action between joists and sheathing is ignored;
2. The CFS joists experience ductile failure under bending
3. Sheathing boards are modeled as Euler-Bernoulli beams, ignoring any torsional or two-way effects
4. Second-order effects caused by large deflections are ignored
5. The simplified load redistribution algorithm described in the Methodology section is used, including all of its assumptions, to permit Monte Carlo simulation for reliability estimation; and
6. Joist failure is defined according to the mean unfactored demand:capacity ratio calculations described in the Methodology section, consistent with AISI S100-12.

Results

Results of the Monte Carlo simulations consist of measures of the system performance as a function of the system effect factor R_{sys} for combinations of the floor system geometry, joist end condition, and live load spatial variation model. This section uses three types of calculation to evaluate component and system failure. The first, code-based (CB) calculation, calculated joist demand based purely on tributary area, replicating as closely as possible the structural behavior implicit in code calculations. The second, elastic analysis (EA), used the computational model to evaluate demand on each joist assuming elasticity of the floor system and no inelastic load redistribution. The only difference between the CB and EA cases is that in the EA case the load was applied to the sheathing boards, which act as continuous beams to elastically share the load between joists, in contrast to the pure tributary areas assumed in CB. The third case, redistribution analysis (RA), used the redistribution algorithm to redistribute loads from overcapacity members.

System Response of Basic Floor Model

Fig. 9 shows how the system reliability index changes when the different analysis methods are used: code-based, elastic load distribution analysis, and inelastic load redistribution analysis, all of which used tributary area load variation and pin-ended joists, which are the loading and boundary conditions most commonly assumed in design. Because increasing values of R_{sys} correspond to decreasing values of the mean joist capacity, rightward shifts of the reliability index curves correspond to an increased system reliability index at a given mean joist capacity or to a lower required mean joist capacity at a given target reliability index. This paper used a system reliability index target of $\beta_{sys} = 2.5$ for the floor system. This value reflects both the current component target reliability β_0 for individual structural members reflected in Section F of AISI S100 (AISI 2012) and the lowest target system reliability reflected in ASCE 7-16, Table 1.3-1 ["Target Reliability (Annual Probability of Failure P_F) and Associated Reliability Indexes (β) for Load Conditions that do not Include Earthquake, Tsunami, or Extraordinary Events"] for nonsudden failures in Risk Category I buildings (ASCE and SEI 2016). An identical analysis could be performed should an alternative value of β_{sys} be selected, although the authors believe that the significant inelastic residual capacity of steel may

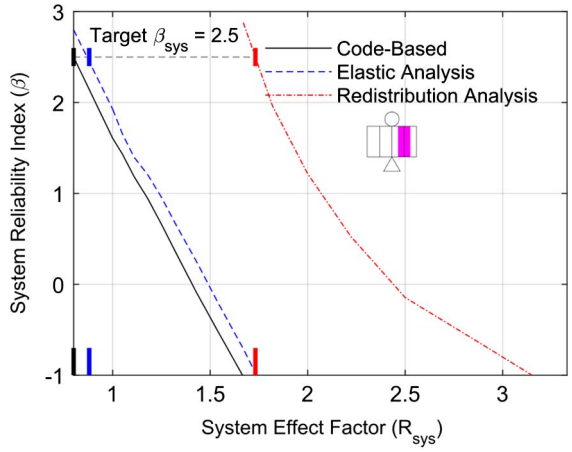

Fig. 9. System reliability index for simplified floor system with pin-ended joists and live load variation by tributary area strips (indicated by icons); horizontal dotted line indicates target reliability for individual joists ($\beta = 2.5$), and marks on x-axis indicate R_{sys} values at which lines cross target reliability; these values of R_{sys} indicate amount that mean joist capacity could be adjusted relative to current component-based designs to achieve target system reliability; $R_{sys} > 1$ implies that joists with lower capacity than dictated by current design procedures can be used without sacrificing system reliability

justify use of the smaller of the system reliability index values given in ASCE 7-16.

Elastic load distribution generally had only a small effect (Fig. 9), and, for this system, always increased the reliability index. Alone, elastic load sharing resulted in an increase of system effect factor of only approximately 0.1, which can be determined by extending a horizontal line rightward from the target system reliability index at $\beta_{sys} = 2.5$ and finding the difference between its points of intersection with the CB reliability index curve and with the EA reliability index curve. Redistribution analysis of the system, however, had a much larger effect, giving a system effect factor increase, read in a similar manner, of approximately 0.9, for a final R_{sys} equal to 1.7.

At R_{sys} equal to 1.0, the CB reliability index is equal to roughly $\beta_{sys} = 1.6$. Given the use of a component reliability of $\beta = 2.5$, it can be surprising to see system reliabilities lower than the component reliability. However, the system is assumed to fail when a single component fails. This is equivalent to treating the system as a series system for which the system reliability is always lower than the component reliability.

Although Fig. 9 shows a significant beneficial system effect, load redistribution can also have a detrimental effect on floor system response. If many joists are loaded to near their capacities and a single joist is overloaded, the redistribution of that load to other joists can lead to a cascading or progressive failure in part or all of the floor system. This detrimental effect will become more pronounced as the mean joist capacity is reduced (increasing R_{sys}). It is also possible that load redistribution will have no effect on the system performance, as when no joists are initially overloaded. Fig. 10 shows how the characteristics of the load redistribution effect shift with increasing R_{sys}.

When R_{sys} is close to 1.0, the EA and RA had no effect on the vast majority of systems, and in no cases was the effect detrimental. In both the EA and RA cases the proportion of Monte Carlo simulated floor systems in which the effect was beneficial increased rapidly as R_{sys} increased, reaching a peak at approximately $R_{sys} = 1.8$. Detrimental effects began to appear at approximately $R_{sys} = 1.6$, and the proportion of systems for which the effect was detrimental then increased steeply and continuously. There are two key points of interest in Fig. 10: the point at which the beneficial effect peaks, and the point at which the detrimental effect first becomes nonzero. This last point is perhaps most important because detrimental effects are equivalent to cascading or progressive collapse, which most code-writing committees will be sensitive to avoiding.

The preceding results all pertain to the simplified floor system with pin-ended joists and tributary area–based load variation. Similar patterns in the dependence of system reliability on system effect factor were observed for fixed end joist conditions, square load variation, and for the CFS-NEES building. Some important differences did appear among the system models, however, and those are described in the next subsection.

Comparison of Floor Systems and Loading Paradigms

The previous subsection refers to the simplified floor system with tributary live load variation and pin-end joists, serving to orient the reader to the methods used in analyzing system reliability effects in a gravity load carrying CFS floor system. Furthermore, that version of the floor system most closely approximates the type of floor system assumed by code calculations. This subsection explores the full parameter space of joist end conditions (pinned or fixed), floor

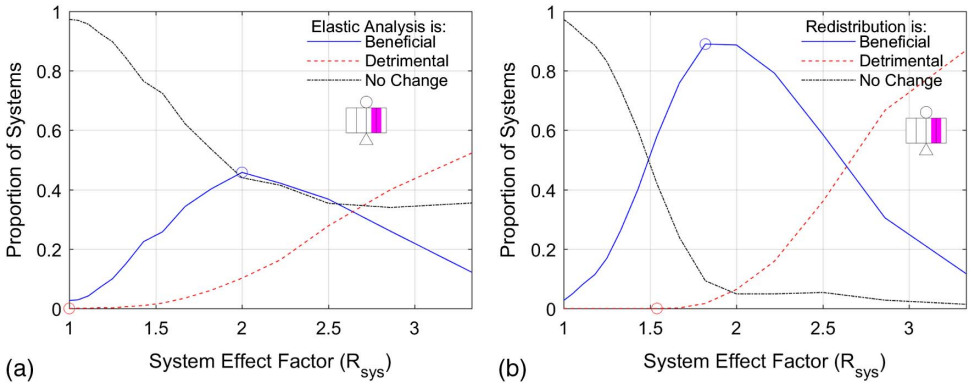

Fig. 10. Beneficial or detrimental system effect for simplified floor system with pin-ended joists and live load variation by tributary area strips (indicated by icons); a circle along beneficial line indicates point of maximum beneficial effect, and a circle along detrimental line indicates last point at which detrimental effect is zero: (a) EA elastic load distribution effects; (b) RA inelastic load redistribution effect

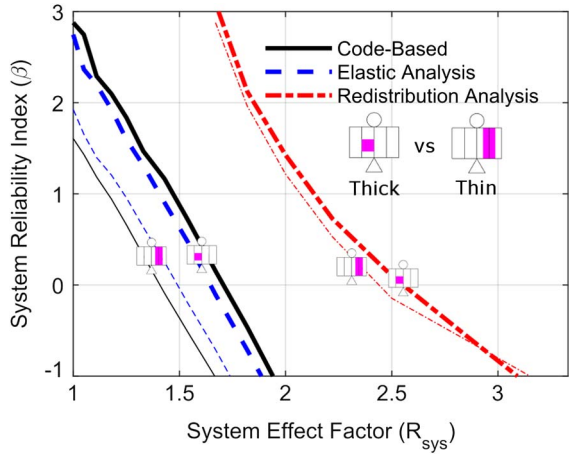

Fig. 11. System reliability for simplified floor system, square load variation pattern [1.22 × 1.22 m (4 × 4 ft)], and pin-ended joists (bold lines); thin lines indicate results for the same system with tributary area strip load variation patterns

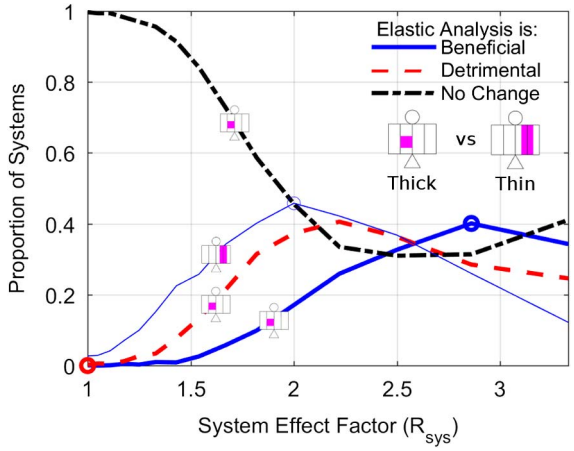

Fig. 12. System effects for simplified floor system with pin-ended joists and square load variation (bold lines); beneficial line is shown only for the equivalent system with strip load variations; beneficial load sharing allows an overloaded joist to shed its load to adjacent joists without causing additional overloads; detrimental load sharing causes progressive or cascading failure of joists as a result of load redistribution

layout (simplified or CFS-NEES), and live load variation (tributary or square).

First, the role of the shape of the live load variation pattern is explored. In the calculations using tributary live load variation, the live load magnitude is assumed constant over the strip-shaped tributary areas of each joist; each area is considered to be an independent, random realization of live load; and all strips are loaded simultaneously. This method is essentially equivalent to ASCE 7 code assumptions. In the square live load calculations the load is assumed constant over 1.22 × 1.22 m (4 × 4 ft) square patches of floor surface area; each square area is considered to be an independent, random realization of live load; and all square patches are loaded simultaneously. Fig. 11 shows how system reliability as a function of R_{sys} differs in the square load variation case from the tributary load variation case. In the figure, the thinner curves represent results for the tributary load variation case and the thicker lines represent results for the square load variation case. In most cases, square load variation patterns lead to a higher reliability at a given value of R_{sys}. This results from the averaging effect that comes from integrating random loading over square patches, which decreases the likelihood of one joist having a significantly higher (or lower) load than its neighbors.

One key difference between the two load variation cases is that the order of the curves changes. For tributary load variation, the order is CB → EA → RA (in order of increasing reliability) where as for the square load variation case, the order is EA → CB → RA, implying that elastic load distribution increases the chances of at least one joist being overloaded in the floor system with the square load variation case. This effect appears because a stronger joint probability relationship between loads on neighboring joists exists in the square load variation case than in the tributary load variation case. In the square load variation case, each loading area extends at least partially over three joists, implying that the loading on each of the three neighboring joists is similar and closely correlated. For a beneficial effect to occur, there must be significantly less load on an overloaded joist's neighbors (i.e., a low correlation), but for a detrimental effect to occur, there must be nearly as much load on an overloaded joist's neighbors (i.e., a high correlation). Therefore the elastic analysis is more likely to be detrimental than beneficial in the square load variation case, as seen in Fig. 12 where, in contrast to Fig. 10(a), elastic analysis is usually more likely to be detrimental than beneficial.

The reliability index curves for the CFS-NEES floor system were in general similar to those for the simplified floor system, but differed notably in the slope of the reliability lines and their position, which was shifted to the right indicating higher reliability indices (Fig. 13). Both of these effects are due to the consistent joist sizes specified throughout the CFS-NEES floor system, regardless of length of loading. This common and sensible design practice leads to significant reserve capacity in many of the joists and means both that initial, as-designed, reliability index is higher than for the simplified floor system and that the reliability decreases more slowly with increasing R_{sys} than for the simplified floor system.

Finally, design calculations typically assume a pinned end condition for floor joists, but joist end connections provide partial restraint. To explore this effect a fully-fixed end condition was compared with the pinned condition (Fig. 14). Fixing the end conditions of the joists, thereby lowering the maximum moment demand, resulted in a small but consistent increase in reliability.

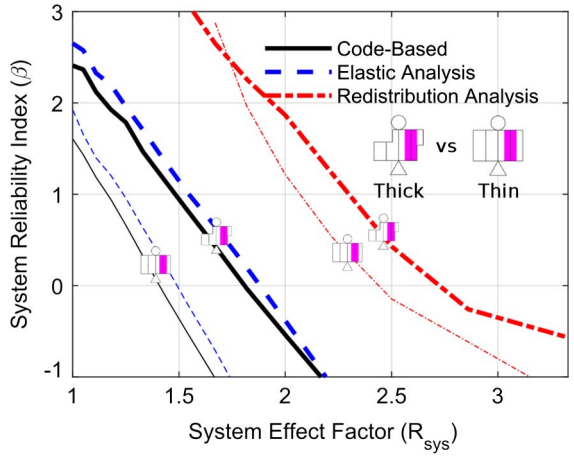

Fig. 13. System reliability index for CFS-NEES floor system with pin ended joists and tributary area strip load variation (bold lines); thin lines indicate results for the equivalent simplified floor system

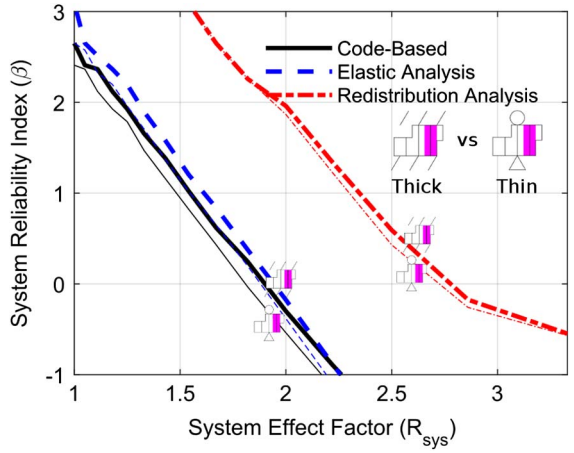

Fig. 14. System reliability index for CFS-NEES floor system with fixed-end joists and tributary area strip load variation (bold lines); thin lines indicate results for the same system with pin-end joists

Fig. 15 shows, for each combination of floor system, joist end condition, and load variation pattern, the values of R_{sys} at which simulations yielded a system reliability index equal to the target system reliability index ($\beta_{sys} = 2.5$); Fig. 9 illustrates the R_{sys} determination. For the CFS-NEES floor system, the presence of reserve capacity in many of the joists means that even code-based calculations for reliability led to values of $R_{sys} > 1.0$. For the simplified floor system, the effect of load redistribution was much larger increases in R_{sys} between code-based and redistribution analysis. Additionally, as discussed in the previous subsection and Fig. 10, the value of R_{sys} at which the first detrimental redistribution effects, corresponding to progressive or cascading failure, is an

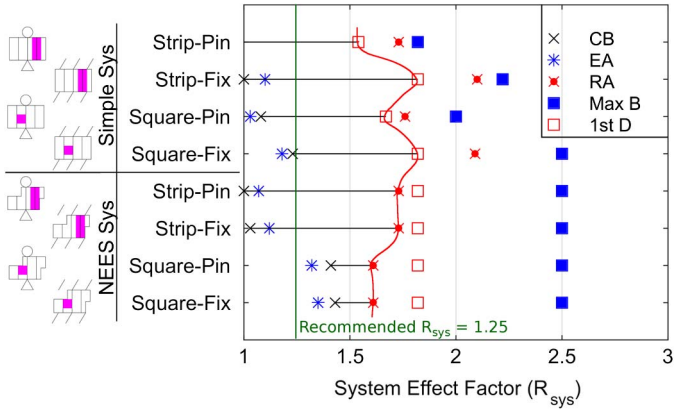

Fig. 15. System effect factor for all eight systems (as indicated by icons at left) at system reliability index of $\beta_{sys} = 2.5$, equal to the AISI target reliability index; for each combination of flooring system, joist end conditions, and load variation pattern; crosses indicate value of R_{sys} at which target reliability of $\beta_{sys} = 2.5$ is met; squares indicate value of R_{sys} at which maximum beneficial system effect and first detrimental system effect occur; curved lines indicate minimum of first detrimental system effect and point at which redistribution analysis falls below $\beta_{sys} = 2.5$, the important point at which redistribution becomes detrimental (i.e., causing a cascading failure) for at least one simulated system realization; CB = code based; EA = elastic analysis; RA = redistribution analysis; Max B = maximum beneficial system effect; 1st D = lowest R_{sys} at which redistribution causes additional failures

important point and is plotted for each system as 1st D. The peak beneficial effect discussed in the previous subsection was always significantly larger, and so was not included in this plot for simplicity. A horizontal line is drawn between the CB point and the minimum of RA and 1st D to indicate the improvement in R_{sys} which results from redistribution. A curved line connects the minimum of RA and 1st D for all systems. The values of R_{sys} obtained over the suite of simulations is quite large, but even the lowest improved value of 1.55 (for the simple system with strip loading and pinned joists) indicates a significant opportunity to achieve greater design efficiency without compromising reliability.

Proposed Repetitive Member Factor

The United States National Design Specifications (NDS) for Wood Construction includes a repetitive member factor that allows a 15% increase in the calculated design capacity of wood joists in a floor system that involves several identical members working in parallel (ANSI and AWC 2012). The structure of cold-formed steel construction is similar, and as shown in this investigation, such a factor would also be appropriate for CFS. In the NDS, the repetitive member factor is intended to include the benefits of three effects: (1) elastic load sharing, (2) postelastic residual capacity, and (3) composite action between sheathing and joists (Rosowsky and Yu 2004). This paper investigated the first two of these effects.

The American Iron and Steel Institute (AISI S100) design specifications follow different conventions than the NDS specifications, so a repetitive member factor would appear differently. It is suggested that such a factor be applied multiplicatively to the resistance factor (ϕ, for LRFD calculations) or the safety factor (Ω, for ASD calculations). In such a scenario, the repetitive member factor R_{sys} would operate as follows:

$$\sum \gamma_i Q_i \le R_{sys}\phi R_n \text{(LRFD)}, \quad \text{or} \quad R = R_{sys}R_n/\Omega \text{ (ASD)} \quad (6)$$

where γ_i = load factors; Q_i = load effects; R_n = capacities; and R = strength.

For a specification committee to adopt this repetitive member factor, they must first choose a target system reliability index (β_{sys}) at which to calculate the value of R_{sys}. If a target system reliability index of $\beta_{sys} = 2.5$ is selected (equal to current component reliability), then, based upon the research in this paper, it is suggested that $R_{sys} = 1.25$ be selected. Although justification could be made for an R_{sys} of up to 1.55, as per the minimum value observed in all simulated systems, a value of 1.25 was selected to be conservative in applying a new design allowance. Furthermore, in some of the floor system failures that would result after application of R_{sys}, multiple joists would exceed their elastic strength, potentially causing greater damage, costs, and consequences than the single joist failure envisioned in current design paradigms. The conservativism of this proposal for R_{sys} parallels that in the accepted value used in the NDS specifications, in which a higher value could also be justified (e.g., Rosowsky and Ellingwood 1991). On the other hand, it should be noted that this study did not include the effect of composite action, which would provide an additional increase in R_{sys}. Other considerations in the floor system behavior that may affect system reliability, but that are not considered here, include the assumption of ductile joist failure, the strength and ability of sheathing boards to distribute loads, and the layout of those sheathing boards. In future work, a more sophisticated model might use the moment-rotation established by Ayhan and Schafer (2017) to replace the elastic-plastic assumption here and develop models for wider classes of CFS joists. Should a different β_{sys} be selected, the resulting value of R_{sys} would need to be

recalculated by a similar method, and higher values of β_{sys} would result in lower values of R_{sys}.

Furthermore, limits involving minimum system size, sheathing type and arrangement, and potentially a minimum cross-section slenderness (for ductile response) must be defined within which the use of an R_{sys} factor would be allowed. For the wood repetitive member factor, the NDS defines these limits by requiring at least three identical dimensioned lumber members spaced no more than 24 in. on-center joined by specified types of load distributing elements. Although further research would be necessary to fully define these limits for cold-formed steel, the beneficial system effect was observed in the simulated joist floor systems of dimensions roughly equal to 14.5×6.5 m (21×48 ft), having standard staggered sheathing boards. Because load is generally unable to redistribute beyond the width of one set of sheathing boards, it is likely that an equal redistribution benefit would be observed on any system with at least two rows of staggered sheathing boards and including at least one half overlap (in these simulations, equal to seven parallel joists).

Conclusions

This paper explored the benefits of repetitive framing to the gravity load carrying capacity of a CFS floor system. Load redistribution simulations accounted for elastic distribution caused by the sheathing board layout and load redistribution after the assumed ductile failure of individual joists. Joist capacities and loading were treated as uncertain and Monte Carlo simulation was used to evaluate the system reliability of the floor system under progressive degrees of reduction of the mean capacity of the joists. The system effect factor $R_{sys} > 1$ was introduced as a means of quantifying the increase in the resistance factor that would result in achieving acceptable system reliability. By exploring two flooring system layouts, two joist end conditions, and two patterns of load variation, the paper showed how values of R_{sys} can vary across floor systems with similar characteristics, but that in all cases $R_{sys} > 1$ showed that a beneficial system effect was present. Based on this research, it is suggested that such a repetitive framing or system effect factor equal to $R_{sys} = 1.25$ be included in the design specifications, which would allow for more-efficient structural systems without compromising overall system reliability.

Acknowledgments

The financial and in-kind support of the American Iron and Steel Institute is gratefully acknowledged, as is the in-kind support of NBM Technologies and the financial support provided by the United States National Science Foundation through grants CMMI-1301033, 1301001, and 1300484. Any opinions, findings, and conclusions or recommendations expressed in this material are those of the authors and do not necessarily reflect the views of the American Iron and Steel Institute, NBM Technologies, or the National Science Foundation.

References

ABAQUS version 6.13 [Computer software]. Dassault Systèmes, Waltham, MA.

Agarwal, A., and Varma, A. H. (2014). "Fire induced progressive collapse of steel building structures: The role of interior gravity columns." *Eng. Struct.*, 58, 129–140.

AISI (American Iron and Steel Institute). (2012). "North American specifications for the design of cold-formed steel structural members." *AISI S100-12*, Washington, DC.

ANSI and AWC (American National Standards Institute and American Wood Council). (2012). "National design specifications for wood construction." *ANSI/AWC NDS 2012*, Leesburg, VA.

ASCE and SEI (Structural Engineering Institute). (2010). "Minimum design loads for buildings and other structures." *ASCE/SEI 7-10*, Reston, VA.

ASCE and SEI (Structural Engineering Institute). (2016). "Minimum design loads for buildings and other structures." *ASCE/SEI 7-16*, Reston, VA.

Ayhan, D., and Schafer, B. W. (2017). "Characterization of in-plane backbone response of cold-formed steel beams." *J. Const. Steel Res.*, 132, 141–150.

Chatterjee, A. (2016). "Structural system reliability with application to light steel-framed buildings." Ph.D. dissertation, Virginia Polytechnic Institute, Blacksburg, VA.

Chatterjee, A., Arwade, S. R., Schafer, B. W., and Moen, C. D. (2017). "System reliability of floor diaphragms framed from cold-formed steel with wood sheathing." *J. Struct. Eng.*, 10.1061/(ASCE)ST.1943-541X.0001958, 04017208.

Collins, M., Kasal, B., Paevere, P., and Foliente, G. C. (2005). "Three-dimensional model of light frame wood buildings. I: Model description." *J. Struct. Eng.*, 10.1061/(ASCE)0733-9445(2005)131:4(676), 676–683.

Dubina, D. (2008). "Behavior and performance of cold-formed steel-framed houses under seismic action." *J. Const. Steel Res.*, 64(7–8): 896–913.

Ellingwood, B. R., and Kinali, K. (2009). "Quantifying and communicating uncertainty in seismic risk assessment." *Struct. Saf.*, 31(2), 179–187.

Fiorino, L., Della Corte, G., and Landolfo, R. (2007). "Experimental tests on typical screw connections for cold-formed steel housing." *Eng. Struct.*, 29(8), 1761–1773.

Foschi, R. O., and Yao, F. Z. (1989). "Reliability analysis of wood I-joists." *Can. J. Civ. Eng.*, 20(4), 564–573.

Fülöp, L. A., and Dubina, D. (2004). "Performance of wall-stud cold-formed shear panels under monotonic and cyclic loading. Part II: Numerical modelling and performance analysis." *Thin-Walled Struct.*, 42(2), 339–349.

Gad, E. F., Duffield, C. F., Hutchinson, G. L., Mansell, D. S., and Stark, G. (1999). "Lateral performance of cold-formed steel-framed domestic structures." *Eng. Struct.*, 21(1), 83–95.

Galambos, T. V., Ellingwood, B. R., MacGregor, J. G., and Cornell, C. A. (1982). "Probability based load criteria: Assessment of current design practice." *J. Struct. Div.*, 108(5), 959–977.

Hendawi, S., and Frangopol, D. M. (1994). "System reliability and redundancy in structural design and evaluation." *Struct. Saf.*, 16(1–2), 47–71.

Iuorio, O., Fiorino, L., and Landolfo, R. (2014). "Testing CFS structures: The new school BFS in Naples." *Thin-Walled Struct.*, 84, 275–288.

Izzuddin, B. A., Vlassis, A. G., Elghazouli, A. Y., and Nethercot, D. A. (2008). "Progressive collapse of multi-storey buildings due to sudden column loss—Part I: Simplified assessment framework." *Eng. Struct.*, 30(5), 1308–1318.

Landolfo, R., Fiorino, L., and Della Corte, G. (2006). "Seismic behavior of sheathed cold-formed structures: Physical tests." *J. Struct. Eng.*, 10.1061/(ASCE)0733-9445(2006)132:4(570), 570–581.

Li, Y., Shen, S., Yao, X., Ma, R., and Liu, F. (2012). "Experimental investigation and design method research on low-rise cold-formed thin-walled steel framing buildings." *J. Struct. Eng.*, 10.1061/(ASCE)ST.1943-541X.0000720, 818–836.

Madsen, R. L., Nakata, N., and Schafer, B. W. (2012). "CFS-NEES building structural design narrative." *Research Rep. No. CFS-NEES-RR01*, CFS-NEES: Advancing Cold-Formed Steel Earthquake Engineering, Baltimore.

MATLAB [Computer software]. MathWorks, Natick, MA.

McGuire, R. K., and Cornell, C. A. (1974). "Live load effects in office buildings." *J. Struct. Div.*, 100(7), 1351–1366.

Moses, F. (1982). "System reliability developments in structural engineering." *Struct. Saf.*, 1(1), 3–13.
Nakata, N., Schafer, B. W., and Madsen, R. L. (2012). "Seismic design of multi-story cold-formed steel buildings: The CFS-NEES archetype building." *Proc., 2012 Structures Congress*, ASCE, Chicago, 1507–1517.
Peterman, K. (2014). "Behavior of full-scale cold formed steel buildings under seismic excitations." Ph.D. dissertation, Johns Hopkins Univ., Baltimore.
Peterman, K., Schafer, B. W., Madsen, R. L., Buonopane, S., and Nakata, N. (2014). "Experimental performance of full-scale cold-formed steel buildings under seismic excitations." *Dataset. Network for earthquake engineering simulation (NEES)*, Purdue Univ., West Lafeyette, IN.
Rashedi, R., and Moses, F. (1988). "Identification of failure modes in system reliability." *J. Struct. Eng.*, 10.1061/(ASCE)0733-9445(1988)114:2(292), 292–313.
Rosowsky, D., and Ellingwood, B. (1991). "System reliability and load sharing effects in light frame wood construction." *J. Struct. Eng.*, 10.1061/(ASCE)0733-9445(1991)117:4(1096), 1098–1116.
Rosowsky, D., and Ellingwood, B. (1992). "Reliability of wood systems subjected to stochastic live loads." *Wood Fiber Sci.*, 24(1), 47–59.
Rosowsky, D. V., and Yu, G. (2004). "Partial factor approach to repetitive-member system factors." *J. Struct. Eng.*, 10.1061/(ASCE)0733-9445(2004)130:11(1829), 1829–1841.
Schafer, B. W. (2015). "NEESR-CR: Enabling performance-based seismic design of multi-story cold-formed steel structures." ⟨www.ce.jhu.edu/cfsnees⟩ (May 12, 2015).
Serrette, R., Encalada, J., Juadines, M., and Nguyen, H. (1997). "Static racking behavior of plywood, OSB, gypsum, and fiberboard walls with metal framing." *J. Struct. Eng.*, 10.1061/(ASCE)0733-9445(1997)123:8(1079), 1079–1086.
Smith, B. H., Arwade, S. R., Schafer, B. W., and Moen, C. D. (2016). "Design component and system reliability in a low-rise cold-formed steel framed commercial building." *Eng. Struct.*, 127, 434–446.
Verrill, S. P., and Kretschmann, D. E. (2010). "Repetitive member factors for the allowable properties of wood products." *Research Paper FPL-RP-657*, U.S. Dept. of Agriculture, Forest Service, Forest Products Laboratory, Madison, WI.